Available online at www.sciencedirect.com
SCIENCE DIRECT®
Estuarine, Coastal and Shelf Science 56 (2003) 369–376
ESTUARINE COASTAL AND SHELF SCIENCE

Inherent and apparent optical properties in coastal waters: a study of the Clyde Sea in early summer

D. McKee[a,*], A. Cunningham[a], J. Slater[a], K.J. Jones[b], C.R. Griffiths[b]

[a]*Department of Physics and Applied Physics, University of Strathclyde, 107 Rottenrow East, Glasgow G4 0NG, Scotland, UK*
[b]*Dunstaffnage Marine Laboratory, P.O. Box 3, Oban, Argyll, PA34 4AD, Scotland, UK*

Received 2 November 2001; received in revised form 1 February 2002; accepted 1 February 2002

Abstract

Profiles of absorption and attenuation coefficients, downward irradiance and upward radiance were measured at 14 stations in the Clyde Sea during May 2000. The absorption coefficient at 676 nm was linearly correlated with chlorophyll concentration ($R^2 = 0.88$), and the ratio of scattering to absorption in this waveband could be used to discriminate between phytoplankton and other suspended material. The radiance and irradiance measurements showed rapid attenuation of blue and red wavelengths near the surface, while the red component was augmented by chlorophyll fluorescence in deeper waters. Throughout the Clyde Sea the relationship between absorption coefficients $a(\lambda)$, scattering coefficients $b(\lambda)$, and diffuse attenuation coefficients for downward irradiance $K_d(\lambda)$ was well described by a function proposed by Kirk (1984). A procedure was devised for retrieving inherent optical properties from measurements of the radiance reflectance and diffuse attenuation coefficient that was able to successfully predict measured absorption coefficients throughout the study area ($R^2 = 0.95$). Backscattering ratios estimated using this procedure varied with depth and location according to changes in the relative concentration of phytoplankton to other particles. Tables of measured inherent and apparent optical properties and derived backscattering ratios for near-surface water are provided for modelling radiative transfer in the Clyde Sea and other coastal areas subject to freshwater influence.
© 2003 Elsevier Science B.V. All rights reserved.

Keywords: Optical measurements; Remote sensing; Reflection profiles; Scattering theory

1. Introduction

The Clyde Sea is a hydrographically complex inlet lying off the west coast of Scotland, which consists of a group of deep fjords to the north and a broad shallow plateau to the south. The area is a region of freshwater influence (Simpson, Sharples, & Rippeth, 1991), where the outflows of the River Clyde and a number of smaller rivers mix with water originating in the Irish Sea and the North Atlantic. Over the years the Clyde Sea has been extensively surveyed and detailed descriptions have been published of its hydrography (Edwards et al., 1986), phytoplankton ecology (Boney, 1986; Tett, Gowen, Grantham, & Jones, 1987), nutrient concentrations (Grantham & Tett, 1993) and suspended particulate material distributions (Balls, 1990). The physical processes linking these factors were investigated by Simpson and Rippeth (1993) and Rippeth and Simpson (1996). Since the Clyde Sea contains a great variety of Case 2 water types in a small area it is an excellent site for studying interactions between physical and biological factors and their influence on optical properties (Bowers, Harker, Smith, & Tett, 2000; McKee, Cunningham, & Jones, 1999). There is a pressing need for such studies as increasing emphasis is placed on the use of airborne and satellite-borne optical sensors for monitoring the status of coastal ecosystems and measuring primary productivity in shelf seas (Bricaud, Morel, & Barale, 1999; Gould, Arnone, & Sydor, 2001; Moore, Aiken, & Lavender, 1999; Tassan, 1994). The deployment of moored optical instrumentation for acquiring time series on coastal mixing, sediment dynamics and phytoplankton growth is also a rapidly developing field (Dickey & Williams, 2001; Gardner

* Corresponding author.
E-mail address: david.mckee@strath.ac.uk (D. McKee).

0272-7714/03/$ - see front matter © 2003 Elsevier Science B.V. All rights reserved.
doi:10.1016/S0272-7714(02)00189-0

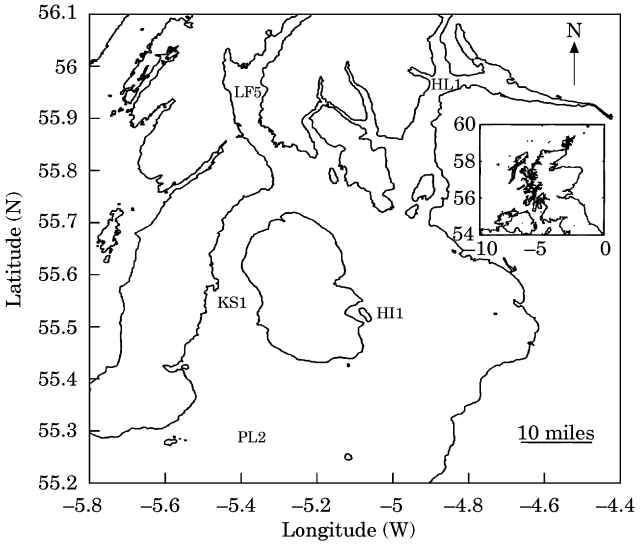

Fig. 1. Map of the Clyde Sea with station positions marked.

et al., 2001). The work presented in this paper seeks to build on our previous knowledge of the Clyde Sea by providing in situ measurements of a range of inherent optical properties and apparent optical properties (IOPs and AOPs) and by investigating the relationships between them.

2. Materials and methods

Data for this paper were collected on a cruise of the R.V. *Calanus* between the 16 and 19 May 2000, during which 14 stations were occupied. For the sake of brevity, we have chosen five stations as being typical of different regions of the Clyde Sea. The positions of these stations are indicated on the map in Fig. 1.

2.1. Hydrographic measurements

Hydrographic measurements were made using a Seabird SBE 9 CTD system equipped with a dissolved oxygen probe, a SeaTech fluorometer and a 25 cm path length SeaTech transmissometer operating at 660 nm. Water samples were collected using a 12-bottle rosette sampler interfaced to the CTD system.

2.2. IOP measurements

A WetLabs ac-9 was used to measure the absorption coefficient (a) and beam attenuation coefficient (c) at the nine wavebands of 10 nm width (FWHM) listed in Table 1. Optical blanks for the ac-9 were regularly measured using ultrapure Millipore water treated with ultraviolet light to break down dissolved organic material. Calibration of the absorption and attenuation sensors remained within the manufacturer's specification (± 0.005 m^{-1}) throughout the cruise. Absorption and attenuation signals at 715 nm were corrected for temperature dependent water absorption (Pegau & Zaneveld, 1993) and a scattering correction algorithm was applied to the absorption measurements (Zaneveld, Kitchen, & Moore, 1994). The data were averaged over 1 m depth intervals using software written in our laboratory, and the scattering coefficient (b) was obtained from the difference between the coefficients of absorption and attenuation. The ac-9 measures absorption and attenuation coefficients relative to pure water, $(a_t - a_w)_\lambda$ and $(c_t - c_w)_\lambda$ where λ denotes waveband and the subscripts t and w refer to 'total' and 'water' coefficients respectively.

2.3. Radiometric measurements and AOP derivation

Downward irradiance (E_d) and upward radiance (L_u) were measured in seven wavebands (10 nm FWHM, as listed in Table 2) across the visible spectrum using a free-falling Satlantic profiling multi-channel radiometer (SPMR). The SPMR was deployed at a distance of at least 20 m from the ship in order to avoid shadowing. The stability of the SPMR and deck reference irradiance sensors was monitored at the start and end of the cruise using a 100 W standard lamp, and the SPMR radiance sensors were checked by using the same lamp to illuminate a Spectralon reflectance target. Over this time all sensors remained within factory specifications.

Table 1
Inherent optical properties, averaged over the top 5 m of the water column

Station	IOP	412 nm	440 nm	488 nm	510 nm	532 nm	555 nm	650 nm	676 nm	715 nm
HL1	$a_t - a_w$	0.534	0.440	0.256	0.203	0.159	0.111	0.057	0.118	0
	$b_t - b_w$	0.774	0.714	0.749	0.745	0.754	0.775	0.727	0.650	0.762
HI1	$a_t - a_w$	0.359	0.274	0.146	0.109	0.085	0.062	0.026	0.045	0
	$b_t - b_w$	0.426	0.384	0.397	0.404	0.404	0.410	0.392	0.366	0.400
PL2	$a_t - a_w$	0.307	0.234	0.123	0.091	0.071	0.051	0.019	0.032	0
	$b_t - b_w$	0.415	0.369	0.372	0.375	0.377	0.378	0.356	0.334	0.350
KS1	$a_t - a_w$	0.312	0.232	0.119	0.089	0.068	0.048	0.017	0.025	0
	$b_t - b_w$	0.395	0.352	0.349	0.345	0.345	0.346	0.317	0.298	0.310
LF5	$a_t - a_w$	0.420	0.330	0.184	0.136	0.106	0.077	0.030	0.053	0
	$b_t - b_w$	0.782	0.742	0.767	0.785	0.789	0.795	0.766	0.727	0.768

Table 2
Apparent optical properties measured just below the surface, and euphotic depths (Z_{eu})

Station	AOP	412 nm	443 nm	491 nm	510 nm	554 nm	665 nm	700 nm	Z_{eu} (m)
HL	K_d	0.733	0.561	0.373	0.337	0.266	0.633	0.728	14
	$R_L \times 10^3$	1.19	1.82	2.74	3.30	4.37	1.71	2.49	
HI1	K_d	0.467	0.329	0.204	0.189	0.170	0.549	0.690	22
	$R_L \times 10^3$	1.36	2.02	2.76	3.07	3.09	1.10	2.00	
PL2	K_d	0.433	0.310	0.216	0.202	0.197	0.557	0.690	23
	$R_L \times 10^3$	1.40	2.10	2.70	2.98	2.80	0.91	1.64	
KS1	K_d	0.416	0.276	0.158	0.149	0.137	0.506	0.627	24
	$R_L \times 10^3$	1.62	2.55	3.60	3.84	3.78	0.92	1.14	
LF5	K_d	0.605	0.457	0.314	0.288	0.255	0.686	0.846	15
	$R_L \times 10^3$	1.54	2.48	3.77	4.61	5.41	1.67	2.74	

Signals from the SPMR were processed using ProSoft, a Matlab module supplied by the manufacturers. Data processing steps included the application of calibration constants, averaging over 1-m deep intervals and deriving diffuse attenuation coefficients (K_d) and radiance reflectances ($R_L = L_u/E_d$).

2.4. Chlorophyll analysis

Chlorophyll samples were filtered through 25 mm GF/F filters and immediately frozen. Once in the laboratory, the filter papers were soaked for 24 h in neutralized 90% acetone and the absorbance of the extract measured in a custom-built spectrophotometer using 1-cm pathlength cuvettes before and after acidification with dilute hydrochloric acid. The trichromatic equations suggested by Jeffrey and Humphrey (1975) were used to convert absorbance spectra to concentrations of chlorophylls, and the Lorenzen (1967) technique was used to obtain concentrations of phaeopigment. All samples were measured in triplicate. The sums of the chlorophyll and phaeopigment concentrations are given as 'total pigment' in the results Section.

2.5. Consistency of IOP and AOP measurements

Given the technical difficulties involved in making accurate optical measurements at sea and the numerous opportunities for introducing systematic errors, it was necessary to devise a method of checking whether the SPMR and ac-9 data were mutually consistent. Kirk (1984) derived a relationship between the mean diffuse attenuation coefficient in the euphotic zone ($\bar{K}_d$) and absorption and scattering coefficients of the form:

$$\bar{K}_d(\lambda) = \frac{[a(\lambda)^2 + (0.425\cos\vartheta_{sw} - 0.19)a(\lambda)b(\lambda)]^{1/2}}{\cos\vartheta_{sw}} \quad (1)$$

where ϑ_{sw} is the solar angle in the water. This angle can be calculated if the solar angle above the water or the latitude, longitude and time of day are known. Eq. (1) is derived from Monte Carlo modelling and assumes that the volume scattering function is adequately described by the Petzold turbid-harbour phase function. It was previously used by Bowers et al. (2000) to test a simple model of absorption and scattering in the Clyde Sea, and can be used to predict diffuse attenuation coefficients from ac-9 measurements of absorption and scattering. The predicted $\bar{K}_d$s can then be compared with those obtained from the SPMR data, and the degree of correlation obtained is a sensitive indicator of the consistency of the in situ IOP and AOP measurements.

2.6. Retrieval of absorption and backscattering coefficients from AOPs

Radiative transfer calculations require knowledge of the volume scattering function (VSF). It is difficult to measure the VSF directly, but a good approximation can be obtained by using analytical scattering functions if the ratio of backscattering to total scattering (b_b/b) is known (Mobley, 1994). Total scattering coefficients (b) were measured by the ac-9, but none of the new submersible instruments for measuring b_b were available at the time of this cruise. However Morel and Gentili (1993) suggested that the ratio of backscattering to absorption (b_b/a) was related to radiance reflectance (R_L) by:

$$R_L(\lambda) \approx 0.094\frac{b_b(\lambda)}{a(\lambda)} \quad (2)$$

This relationship is relatively insensitive to solar angle. In addition Gordon (1989) proposed that:

$$K_d(\lambda) \approx 1.0395\frac{a(\lambda) + b_b(\lambda)}{\cos(\vartheta_{sw})} \quad (3)$$

Eqs. (2) and (3) can be combined to provide estimates of the inherent optical properties $a(\lambda)$ and $b_b(\lambda)$ from measurements of the apparent optical properties R_L and K_d:

$$a(\lambda)_{est} \approx \frac{K_d(\lambda)\cos\vartheta_{sw}}{1.0395\left[\frac{R_L(\lambda)}{0.083} + 1\right]} \quad (4)$$

and

$$b_b(\lambda)_{est} \approx \frac{K_d(\lambda)\cos\vartheta_{sw}}{1.0395\left[\frac{0.083}{R_L(\lambda)}+1\right]} \quad (5)$$

Since $K_d(\lambda)$ and $R_L(\lambda)$ can be derived from SPMR measurements and ϑ_{sw} is known for each station, it is possible to use Eqs. (4) and (5) to estimate the absorption and backscattering coefficients. The procedure can be tested by comparing the estimated absorption coefficients with those actually measured, and backscattering ratios can be obtained by dividing the backscattering coefficients estimated by Eq. (5) by the total scattering coefficients measured by the ac-9.

3. Results

3.1. Inherent optical properties

Fig. 2 shows scattering and absorption spectra for depths representing the surface, middle and bottom layers of station LF5. The absorption coefficients ranged from 0.02 to 0.45 m^{-1}, and showed a general decrease from blue to red wavelengths which is typical of Scottish coastal waters. The surface water showed a distinct absorption peak at 676 nm attributable to phytoplankton chlorophyll, which had a measured concentration of 2 mg m^{-3}. The blue chlorophyll peak was masked by the absorption of other particles and coloured dissolved organic matter. Scattering coefficients varied between 0.5 and 1.0 m^{-1}, with the highest values in the deep water where greater quantities of suspended material were present. Scattering in the surface layer had a lower average spectral slope than in deeper water, and showed minima at the red and blue phytoplankton absorption peaks attributable to Kettler-Helmholtz effects (Stramski, Morel, & Bricaud, 1988). Knowledge of near-surface absorption and scattering coefficients is essential for radiative transfer calculations of remote sensing reflectance. Table 1 provides average values of ac-9 absorption and scattering for the top 5 m of the water column at selected stations, and indicates the range encountered in the Clyde Sea in early summer.

3.2. Inherent optical properties and seawater constituents

Fig. 3 shows the absorption coefficient at 676 nm (with the pure water value subtracted) plotted against extracted photopigment concentration for all fourteen stations and for a full range of depths. The high value of the regression coefficient ($R^2 = 0.88$) indicates that the two variables are well correlated and that absorption at 676 nm can be used to predict chlorophyll concentration with an accuracy of around 1 mg m^{-3}. This is particularly useful for interpolating between data from widely separated water samples when continuous profiles of chlorophyll concentration are required. It is interesting to note that a plot of stimulated fluorescence against total pigment concentration produced an R^2 value of only 0.7. The relationship between absorption $(a_t-a_w)_{676}$ and scattering $(b_t-b_w)_{676}$ in the 676 nm waveband for station LF5 is shown in Fig. 4. Measurements made above and below a depth of 20 m (the base of the pycnocline) fall into separate clusters. The linear relationship between $(b_t-b_w)_{676}$ and $(a_t-a_w)_{676}$ in the surface layer indicates that scattering is mainly due to phytoplankton and associated particles. Below the pycnocline, however, scattering is essentially independent of

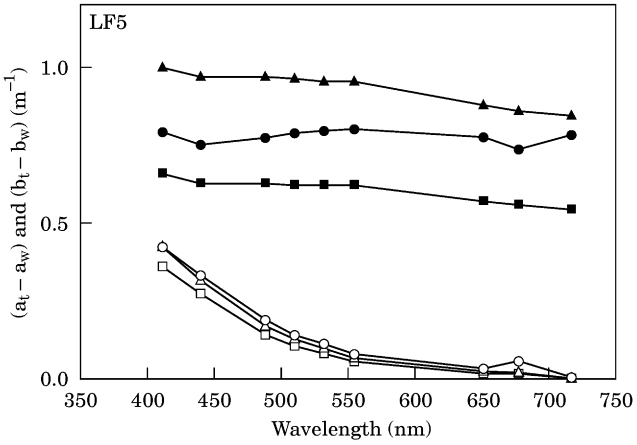

Fig. 2. ac-9 absorption and scattering spectra from selected depths at station LF5. All coefficients are relative to water and have been adjusted for temperature-dependent water absorption and corrected for scattering errors. ○ *a* 1 m, □ *a* 50 m, △ *a* 100 m, ● *b* 1 m, ■ *b* 50 m, ▲ *b* 100 m.

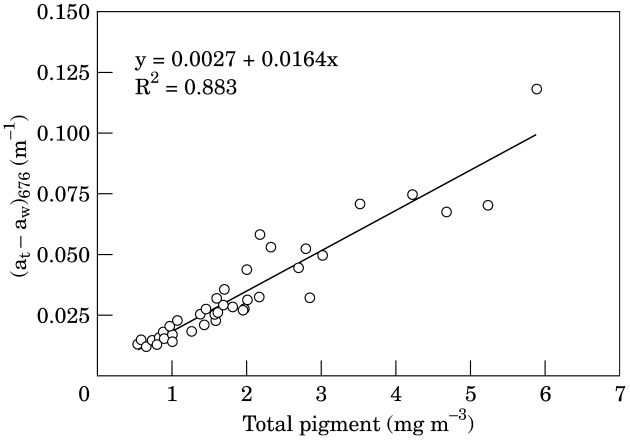

Fig. 3. ac-9 absorption coefficients measured at 676 nm correlate well with total pigment concentrations for all depths and locations sampled in the Clyde Sea.

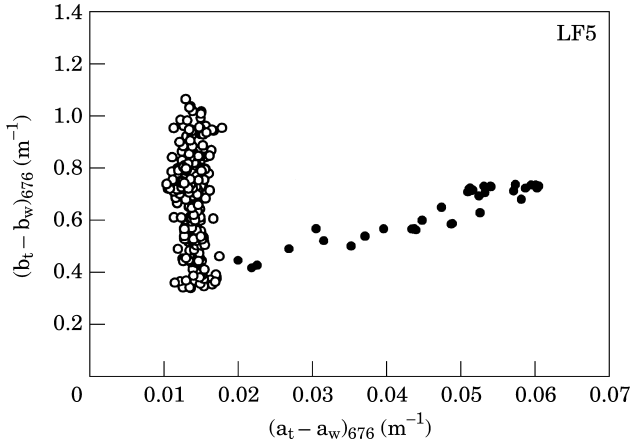

Fig. 4. The bifurcation in the plot of ac-9 scattering against absorption at 676 nm indicates that the pycnocline at 20 m separates phytoplankton dominated surface waters from deeper waters with varying concentrations of detrital material. All data come from a single profile measured at station LF5. ● 0–20 m, ○ >20 m.

chlorophyll absorption and is presumably dominated by particles other than phytoplankton cells.

3.3. In situ radiometry

SPMR measurements of downward irradiance (E_d) and upward radiance (L_u) at station LF5 are illustrated in Fig. 5. Both plots show a rapid attenuation of blue and red wavelengths with depth and a more gradual reduction of green wavelengths. Below 10 m however, E_d and L_u are higher in magnitude at 700 nm than at 665 nm in spite of the rapid increase in water absorption at the red end of the spectrum. This feature is due to the internal generation of red photons by phytoplankton fluorescence. It indicates that the effects of inelastic processes must be taken into account in deriving apparent optical properties from in situ radiometric measurements. Near surface values of K_d and R_L for the five selected stations are given in Table 2, together with estimates of euphotic depth (Z_{eu}) derived from the irradiance measurements.

3.4. Relationships between inherent and apparent optical properties

The results of the previous section show that Eqs. (1)–(3) should be treated with caution since they neglect the effect of inelastic processes on the under-water light field. We have therefore limited our analysis of relationships between apparent and inherent optical properties in the Clyde Sea to the blue-green portion of the spectrum. Fig. 6 shows diffuse attenuation coefficients calculated using Eq. (1) and absorption and scattering coefficients from Table 1 with pure water values added (Pope & Fry, 1997) plotted against the measured diffuse attenuation

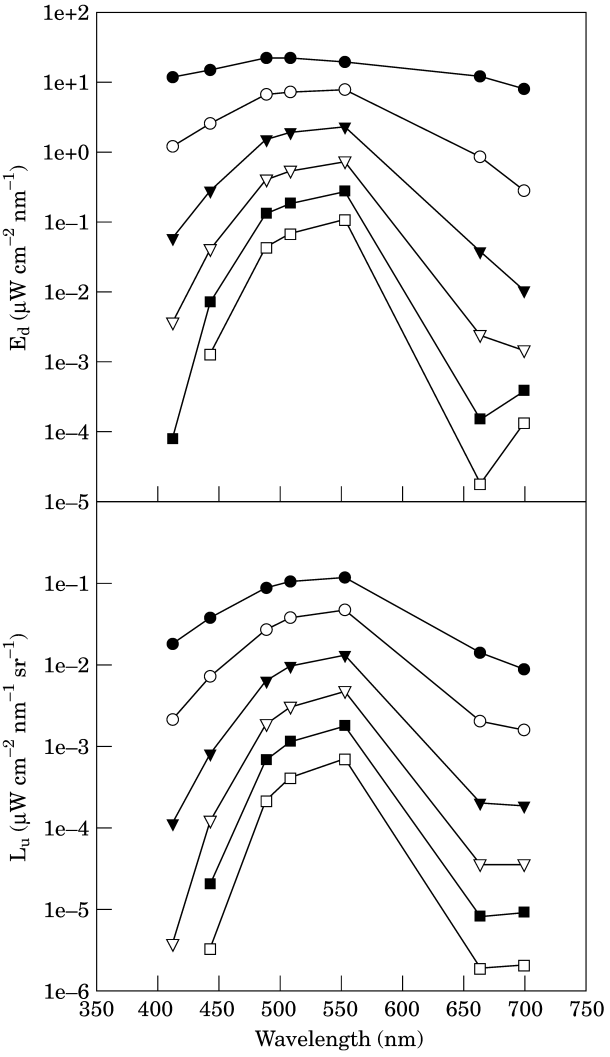

Fig. 5. Downward irradiance and upward radiance signals at seven wavelengths measured using a SPMR at station LF5. Note that light levels at 700 nm decrease with depth more slowly than at 665 nm due to the effect of chlorophyll fluorescence. ● 1 m, ○ 5 m, ▼ 10 m, ▽ 15 m, ■ 20 m, □ 25 m.

coefficients listed in Table 2. The plot shows a strong relationship between predicted and measured diffuse attenuation coefficients, with a correlation coefficient of greater than 0.96 and a gradient close to 1. It is concluded that Kirk's relationship holds remarkably well for this data set and that the IOP and AOP measurements are mutually consistent and free of systematic errors.

Fig. 7 shows absorption coefficients calculated from Eq. (4) plotted against measured absorption coefficients (ac-9 absorption plus absorption by water) for all 14 of the stations occupied during the cruise, all depths for which K_d and R_L could be obtained and the five wavelengths for which instrument detector wavebands were reasonably matched. The data cover a wide range of locations, depths up to 30 m and times of day from early morning to shortly before sunset. The excellent

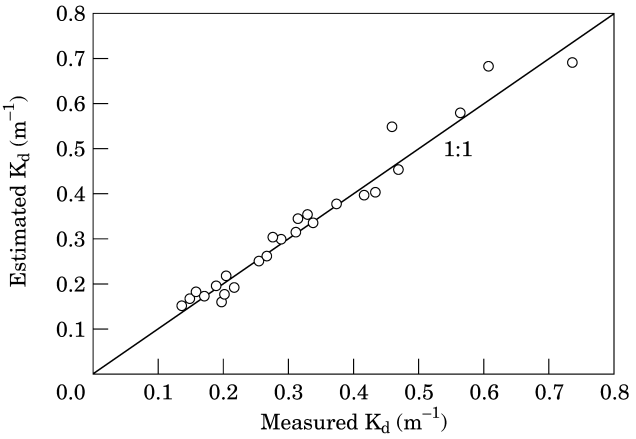

Fig. 6. Values of diffuse attenuation coefficient derived from ac-9 scattering and absorption values correlate well with SPMR measurements.

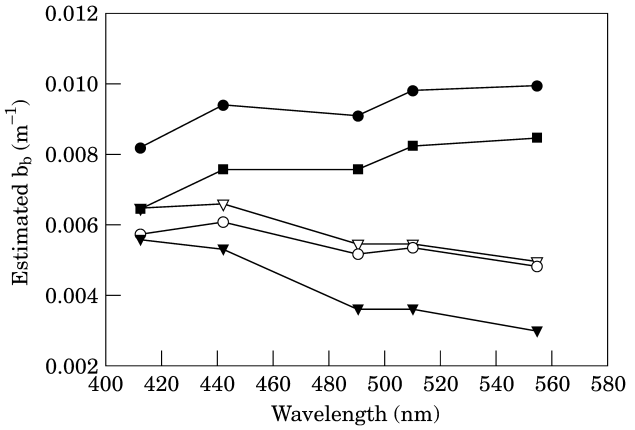

Fig. 8. Values of backscattering coefficient estimated from SPMR derived AOPs using Eq. (5). Spectra are for surface waters at the five stations indicated in Fig. 1. ● HL1, ○ HI1, ▼ PL2, ▽ KS1, ■ LF5.

agreement between estimated and measured absorption coefficients supports the assumptions involved in deriving Eqs. (4) and (5) and suggests that it might be possible to use Eq. (5) to retrieve estimated backscattering coefficients. Examples of backscattering spectra obtained in this way are shown in Fig. 8. When combined with ac-9 measurements of $b(\lambda)$ these spectra give estimates of backscattering ratios which are listed in Table 3. The range of values obtained (0.008 to 0.018) is consistent with the value of 0.013 measured by Petzold in coastal ocean water. The estimated backscattering ratio is plotted as a function of depth for station LF5 in Fig. 9, which shows relatively low values in the surface layer and significantly higher values below the pycnocline. The accompanying profile of absorption at 676 nm (previously shown to be a quantitative measure of chlorophyll concentration) shows that the increase in the backscattering ratio below the pycnocline is accompanied by a decrease in the phytoplankton concentration. Other studies also suggest that phytoplankton exhibit relatively low backscattering ratios compared to other marine particles (Ahn, Bricaud, & Morel, 1995; Stramski & Kiefer, 1991; Stramski & Mobley, 1997).

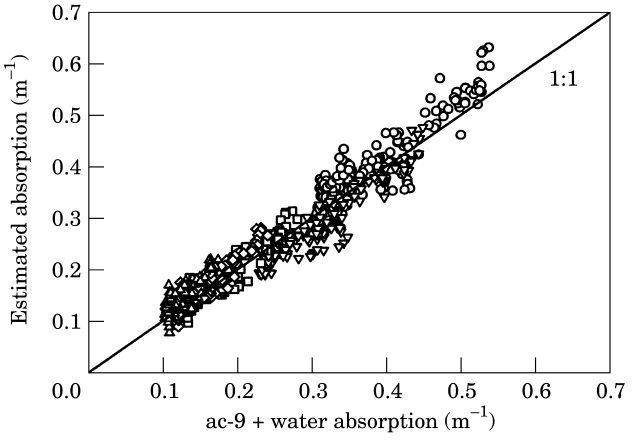

Fig. 7. Estimates of total absorption coefficient derived from Eq. (4) correlate well with total absorption coefficients based on ac-9 measurements. ○ 412 nm, ▽ 442 nm, □ 490 nm, ◇ 510 nm, △ 554 nm.

4. Discussion

The data presented here show that IOP measurements can provide useful quantitative information on the distribution and classification of suspended material in coastal waters. For example, absorption at 676 nm was found to be a better indicator of phytoplankton distribution than stimulated fluorescence (Fig. 3) and the ratio of scattering to absorption could be used to discriminate between phytoplankton and other particulate material (Fig. 4). Measurements of AOP's can be used to check for systematic errors in IOP measurements and to determine parameters of biological interest such as euphotic depths. They also provide an indication of whether the water column can be adequately sampled by optical remote sensing. In the Clyde Sea, diffuse attenuation coefficients for downward irradiance varied from 0.14 to 0.85 m^{-1}, corresponding to first optical depths as shallow as 1 m and not deeper than 7 m. Since nearly all of the water-leaving radiance originates from

Table 3
Estimated backscattering ratios, averaged over the top 5 m of the water column

Station	b_b/b 412 nm	b_b/b 442 nm	b_b/b 490 nm	b_b/b 510 nm	b_b/b 554 nm
HL1	0.011	0.013	0.013	0.013	0.013
HI1	0.013	0.016	0.013	0.013	0.012
PL2	0.013	0.013	0.010	0.010	0.008
KS1	0.015	0.018	0.014	0.014	0.013
LF5	0.009	0.011	0.011	0.012	0.012

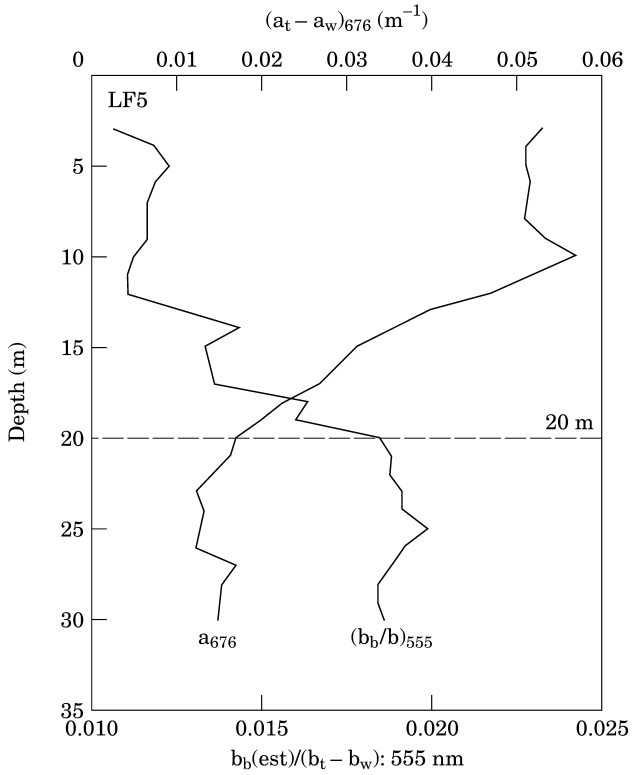

Fig. 9. High chlorophyll (high a_{676}) surface waters have a lower backscattering ratio at 555 nm than deeper waters where detrital particles dominate scattering.

the first optical depth, it follows that optical remote sensing will produce information on a layer that is significantly shallower than the average depth of the pycnocline. In other cruises in this region significant phytoplankton populations have been found towards the base of the pycnocline that would be invisible to airborne or satellite remote sensing. The fact that in situ measurements have confirmed a theoretical relationship between IOPs and AOPs in optically complex coastal waters is interesting for several reasons. First, it indicates that relatively simple bio-optical models (such as the one developed by Bowers et al., 2000) can be used to describe these Case 2 waters. Second, it provides a means of estimating backscattering coefficients that appear to be realistic and consistent with other estimates for coastal waters (e.g. Stramska, Stramski, Mitchell, & Mobley, 2000). The average backscattering ratio (0.013) calculated in this way is identical to Petzold's coastal water measurement. Third, it provides a computational route from remote sensing reflectance via diffuse attenuation coefficients to inherent optical properties. This is potentially valuable for interpreting satellite imagery of coastal waters, where the development of image processing algorithms is particularly challenging. The set of optical properties measured in the Clyde Sea may prove useful for exploratory optical modelling of fjords and other areas subject to significant freshwater input such as the Baltic Sea. Such models provide a basis for developing the algorithms required for interpreting data from the new generation of high resolution ocean colour sensors (e.g. Moore et al., 1999). We hope to present work of this nature in a subsequent paper.

Acknowledgements

This work was funded by the UK Natural Environment Research Council, and made possible by the generous assistance provided by the crew of RV *Calanus*.

References

Ahn, Y.-H., Bricaud, A., & Morel, A. (1995). Light backscattering efficiency and related properties of some phytoplankters. *Deep Sea Research 39*, 1835–1855.

Balls, P. W. (1990). Distribution and composition of suspended particulate material in the Clyde estuary and associated sea lochs. *Estuarine, Coastal and Shelf Science 30*, 475–487.

Bowers, D. G., Harker, G. E. L., Smith, P. S. D., & Tett, P. (2000). Optical properties of a region of freshwater influence (the Clyde Sea). *Estuarine, Coastal and Shelf Science 50*, 717–726.

Boney, A. D. (1986). Seasonal studies on the phytoplankton and primary production in the inner Firth of Clyde. *Proceedings of the Royal Society of Edinburgh, B 90*, 203–222.

Bricaud, A., Morel, A., & Barale, V. (1999). MERIS potential for ocean colour studies in the open ocean. *International Journal of Remote Sensing 20*, 1757–1769.

Dickey, T. D., & Williams, A. J. (2001). Interdisciplinary ocean process studies on the New England shelf. *Journal of Geophysical Research-Oceans 106*, 9427–9434.

Edwards, A., Baxter, M. S., Ellet, D. J., Martin, J. H. A., Meldrum, D. T., & Griffiths, C. R. (1986). Clyde Sea hydrography. *Proceedings of the Royal Society of Edinburgh, B 90*, 67–83.

Gardner, W. D., Blakey, J. C., Walsh, J. D., Richardson, M. J., Pegau, W. S., Zaneveld, J. R. V., Roesler, C., Gregg, M. C., MacKinnon, J. A., Sosik, H. M., & Williams, A. J. (2001). Optics, particles, stratification and storms on the New England continental shelf. *Journal of Geophysics Research—Oceans 106*, 9473–9497.

Gordon, H. R. (1989). Can the Lambert-Beer law be applied to the diffuse attenuation coefficient of ocean water? *Limnology and Oceanography 34*, 1389–1409.

Gould, R. W., Arnone, R. A., & Sydor, M. (2001). Absorption, scattering and remote sensing reflectance relationships in coastal waters: testing a new inversion algorithm. *Journal of Coastal Research 17*, 328–341.

Grantham, B., & Tett, P. (1993). The nutrient status of the Clyde Sea in winter. *Estuarine, Coastal and Shelf Science 36*, 449–462.

Jeffrey, S. W., & Humphrey, G. F. (1975). New spectrophotometric equations for determining chlorophylls *a*, *b*, c_1 and c_2 in higher plants, algae and natural phytoplankton. *Biochemie Physiologie Pflanzen 167*, 191–194.

Kirk, J. T. O. (1984). Dependence of relationship between inherent and apparent optical properties of water on solar altitude. *Limnology and Oceanography 29*, 350–356.

Lorenzen, C. J. (1967). Determination of chlorophyll and phaeopigments: spectrophotometric equations. *Limnology and Oceanography 12*, 343–346.

McKee, D., Cunningham, A., & Jones, K. (1999). Simultaneous measurements of fluorescence and beam attenuation: instrument

characterization and interpretation of signals from stratified coastal waters. *Estuarine, Coastal and Shelf Science 48*, 51–58.

Mobley, C. D. (1994). *Light and water* (pp. 100). London: Academic Press.

Moore, G. F., Aiken, J., & Lavender, S. J. (1999). The atmospheric correction of water colour and the quantitative retrieval of suspended particulate matter in case II waters: application to MERIS. *International Journal of Remote Sensing 20*, 1713–1733.

Morel, A., & Gentili, B. (1993). Diffuse reflectance of oceanic waters: II bi-directional aspects. *Applied Optics 32*, 6864–6879.

Pegau, W. S., & Zaneveld, J. R. V. (1993). Temperature-dependent absorption of water in the red and near-infrared portions of the spectrum. *Limnology and Oceanography 38*, 188–192.

Pope, R. M., & Fry, E. S. (1997). Absorption spectrum (380–700 nm) of pure water: II. Integrating cavity measurements. *Applied Optics 36*, 8710–8723.

Rippeth, T. P., & Simpson, J. H. (1996). The frequency and duration of episodes of complete vertical mixing in the Clyde Sea. *Continental Shelf Research 16*, 933–947.

Simpson, J. H., & Rippeth, T. P. (1993). The Clyde Sea: a model of the seasonal cycle of stratification and mixing. *Estuarine, Coastal and Shelf Science 37*, 129–144.

Simpson, J. H., Sharples, J., & Rippeth, T. P. (1991). A prescriptive model of stratification induced by freshwater run-off. *Estuarine, Coastal and Shelf Science 33*, 23–35.

Stramska, M., Stramski, D., Mitchell, B. G., & Mobley, C. D. (2000). Estimation of the absorption and backscattering coefficients from in-water radiometric measurements. *Limnology and Oceanography 45*, 628–641.

Stramski, D., & Kiefer, D. A. (1991). Light scattering by micro-organisms in the open ocean. *Progress in Oceanography 28*, 343–383.

Stramski, D., & Mobley, C. D. (1997). Effects of microbial particles on ocean optics: a database of single particle optical properties. *Limnology and Oceanography 42*, 538–549.

Stramski, D., Morel, A., & Bricaud, A. (1988). Modeling the light attenuation and scattering by spherical phytoplanktonic cells: a retrieval of the bulk refractive index. *Applied Optics 27*, 3954–3956.

Tassan, S. (1994). Local algorithms using SeaWiFS data for the retrieval of phytoplankton, pigments, suspended matter, and yellow substance in coastal waters. *Applied Optics 33*, 2369–2378.

Tett, P., Gowen, R., Grantham, B., & Jones, K. (1987). The phytoplankton ecology of the Firth of Clyde sea-lochs Striven and Fyne. *Proceedings of the Royal Society of Edinburgh B 90*, 223–238.

Zaneveld, J. R. V., Kitchen, J. C., & Moore, C. (1994). The scattering error correction of reflection-tube absorption meters. *Ocean Optics XII SPIE* Vol. *2258*, 44–55.